IEEE Access
Multidisciplinary ⋮ Rapid Review ⋮ Open Access Journal

Received January 25, 2021, accepted February 11, 2021, date of publication February 16, 2021, date of current version February 24, 2021.

Digital Object Identifier 10.1109/ACCESS.2021.3059710

Effects of Machine Instability Feedback on Safety During Digging Operation in Teleoperated Excavators

MASARU ITO[1], CHIAKI RAIMA[2], SEIJI SAIKI[3], YOICHIRO YAMAZAKI[3], AND YUICHI KURITA[1], (Member, IEEE)

[1]Graduate School of Advanced Science and Engineering, Hiroshima University, Hiroshima 739-8527, Japan
[2]Office of Academic Research and Industry-Academia-Government and Community Collaboration, Hiroshima University, Hiroshima 739-8527, Japan
[3]Kobelco Construction Machinery Company Ltd., Tokyo 141-8626, Japan

Corresponding author: Masaru Ito (itoma@hiroshima-u.ac.jp)

ABSTRACT Teleoperated excavators have a risk of overturning or falling when digging because it is more difficult to receive information regarding the machine posture and the work object condition than in the case of actual machine boarding. In this study, the machine instability derived from the attachment posture and the digging reaction force has been proposed. In addition, for feedback regarding the machine instability to the operator, an intuitive visual presentation method using a meter is proposed. To verify the effect of the proposed machine instability feedback, an excavation operation simulator was constructed, and an experiment was conducted. As a result, by using the machine instability feedback, it was confirmed that digging could be performed without generating the tilting and forward movements of the machine body, and that the ratio of the time during which the machine instability exceeded 100% decreased, while the productivity remained constant. Additionally, by verifying the effect of the subject experiment, even in the actual teleoperated excavator, it was confirmed that the work could be conducted without generating a greater tilting of the machine body, while maintaining productivity. Therefore, the possibility of working safely in the teleoperated excavator using machine instability feedback was clarified.

INDEX TERMS Hydraulic excavator, man-machine systems, teleoperation, unmanned construction, user-interfaces.

I. INTRODUCTION

Hydraulic excavators are used in various works such as excavation and dismantling. In recent years, teleoperated excavators have been applied in fields that are challenging for humans to enter, such as disaster fields [1]. However, mainstream teleoperated excavators [2] have problems regarding work efficiency and safety.

The work efficiency of a teleoperated excavator is lower than that of a boarding operation because of the delay, and difficulty in understanding the worksite conditions. Additionally, with regard to safety, it is challenging to receive information regarding the posture of the machine and the condition of the work object compared to when on board the actual machine [3], so there is a risk of overturning. Especially in the case of excavation, if the reaction force received from the soil increases, the machine body moves depending on the posture of the attachment, and the risk of overturning increases when operated on irregular grounds and uplands. Eliminating such conditions is thus desirable.

According to Sakaida *et al.* [4], it is suggested that the skilled operator operates the excavator while controlling the load to the bucket according to the change in the posture of the bucket. Thus, it is assumed that the operator estimates the load applied to the machine from the slight change in the tilt of the machine as perceived by the operator, and then the difference between the maximum load that the machine can sustain without the machine body moving and the current load, that is, the load margin; the operator changes the operation when the load margin is small to dig without moving the machine body. As information regarding the machine tilt is received by the teleoperated excavator using monitors without direct visibility, it is difficult for the operator to estimate the load margin; thus, the risk of tipping over and falling is high. Therefore, it is necessary to consider a method that provides information to the teleoperated excavator operator regarding machine posture and the load applied to the machine.

The associate editor coordinating the review of this manuscript and approving it for publication was Giuseppe Desolda.

As a system for feeding back the movement of the excavator to the operator, Zhao *et al.* [5] and the authors [6] researched the feedback of tilt information of the excavator body using a motion base. It is possible to feel the movement of the machine; therefore, the operator could estimate the load acting on the bucket. However, there is a problem in that expensive actuators and controllers are required to reproduce slight tilting. Additionally, the introduction of force feedback has also been studied to provide feedback on the digging reaction force. For example, Parker *et al.* [7] and Lawrence *et al.* [8] used a mounted force feedback operation lever for the excavator. Ahn [9], Li [10], and Truong *et al.* [11] developed a force feedback operation lever for a teleoperated excavator. Gong *et al.* [12] and Hou and Zhao [13] developed a force feedback system in the case of using a fork attachment. Huang *et al.* [14] enabled the discrimination of the hardness of an object grasped by a fork attachment using an operation system that combines force and visual feedback. Zareinia and Sepehri [15] designed a control scheme for a haptic device that provides haptic force based on the position error between the displacements of the master and the slave. Lampinen *et al.* [16] designed a full-dynamics-based bilateral force-reflected teleoperation for hydraulic manipulators. Carvalho *et al.* [17] proposed a force feedback strategy using a 3D haptic device for teleoperated excavators. Haptic feedback has also been studied [18]–[21]. However, it is not easy to estimate the load margin from only the digging reaction force information because this margin changes depending on the attachment posture. In addition, the installation of the force and haptic feedback has a problem in which the operation feeling may be changed for the operator who usually works on board. To overcome this problem, there is a study by Tanimoto *et al.* [22], which provides assistance while maintaining the operation feeling; however, it is difficult to adapt to excavation work without an ideal trajectory. Therefore, in this study, we aimed to change the operation of the operator without changing the operation feeling by adding information presentation to the operator.

On the other hand, regarding the safety of teleoperated excavators, some studies have proposed tip-over prevention control using a static compensation zero moment point algorithm [23] and by predicting the center of gravity and the zero moment point [24]. These studies focused on improving safety when operating the attachment, but not on the excavation. Research on improving safety during digging operations has not been conducted thus far.

Herein, the operator is presented with the amount of the load margin. Thus, it is expected that the operator is aware of the load margin available, leading to safe digging operation. In this study, machine instability derived from the attachment posture and the digging reaction force is proposed. In addition, as a method for providing feedback about the machine instability to the operator, a visual presentation method using a meter is proposed, so that the amount of load margin can be intuitively understood. This study verified that the machine instability feedback could improve the safety during digging work using a teleoperated excavator and how work performance would change.

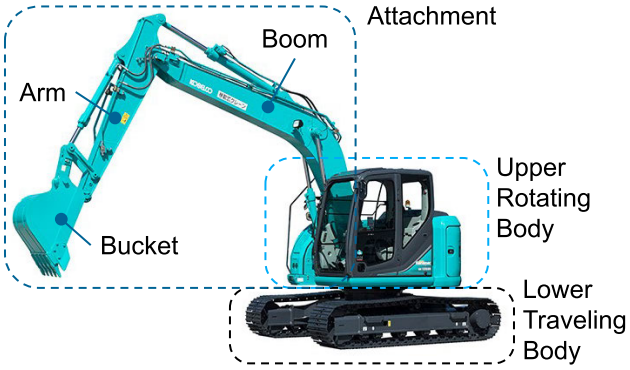

FIGURE 1. Parts of hydraulic excavator.

The preliminary experimental results based on the simulation experiments were explained in International Conference on Human System Interaction (HSI) 2020 [25]. The new contributions of this paper are the subject experiments using an actual teleoperated excavator and investigation and an evaluation of the proposed method based on the results of both the simulator and the actual teleoperated excavator.

This paper is organized as follows. Section II introduces the definition of the proposed machine instability. Section III describes the digging operation simulator developed for the verification of the effect of the machine instability feedback and the results of the verification using the simulator. Section IV describes the results of the verification of the effect of machine instability feedback on actual teleoperated excavators. Section V describes the general discussion and Section VI describes the conclusions drawn from this study.

II. DEFINITION OF MACHINE INSTABILITY

A hydraulic excavator carries out digging work by operating an attachment, consisting of a boom, an arm, and a bucket (Fig. 1). When the reaction force from the digging object increases, the excavator body starts to move depending on the posture of the attachment. For safe operation, it is desirable to eliminate this condition while digging. Therefore, it is proposed a parameter, the machine instability. Machine instability is an index of the excavator condition with the condition when the excavator body starts to move which is assumed to be 100%, and it derived from the attachment posture and the digging reaction force. Two instabilities were considered: the behavior of tilting around the rear end of the lower traveling body as the center of rotation, as shown in Fig. 2a, and the behavior of the body being dragged forward, as shown in Fig. 2b. The value that is greater between these two instabilities is defined as machine instability. In this study, it is assumed that the machine is installed on horizontal ground. Machine motion in the lateral direction and the weight of the attachment are not considered.

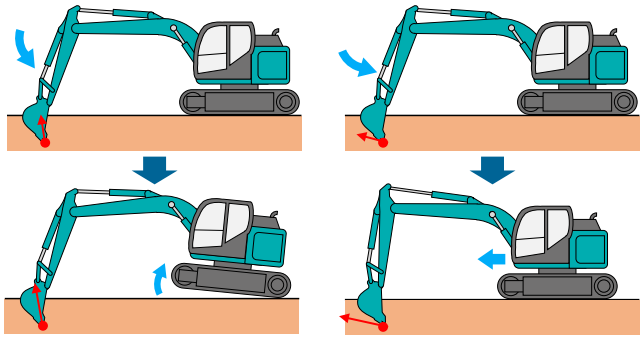

(a) Upward direction. (b) Forward direction.

FIGURE 2. Example of machine behavior when digging reaction force is large.

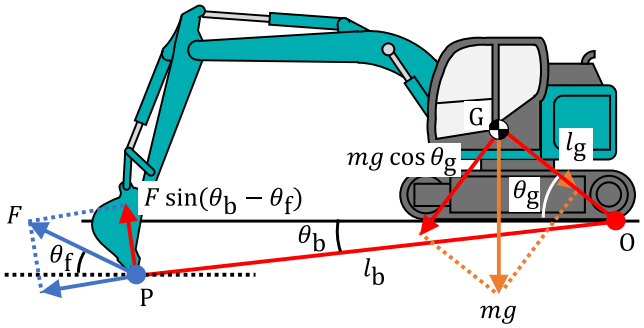

FIGURE 3. Moments of force around rear end of lower traveling body ground surface.

A. UPWARD INSTABILITY

As shown in Fig. 3, considering the moment when the rear end of the lower traveling body is the center of rotation, O, the moment in the counterclockwise direction caused by the machine weight M_m is given by

$$M_m = l_g \cdot mg\cos\theta_g \tag{1}$$

where m is the machine weight, l_g is the distance from O to the center of gravity of the machine weight, G, θ_g is the angle between the ground and l_g, and g is the gravitational acceleration.

The clockwise moment M_f caused by the digging reaction force is given by

$$M_f = l_b \cdot F\sin(\theta_b - \theta_f) \tag{2}$$

where F is the digging reaction force, θ_f is the angle between the digging reaction force direction and the ground, l_b is the distance from O to the digging reaction point, P, and θ_b is the angle between the ground and l_b.

From (1) and (2), the condition under which the machine is lifted is $M_f > M_m$. Thus, the upward instability I_{up} (%) is defined as

$$I_{up} = \frac{M_f}{M_m} \cdot 100. \tag{3}$$

If $I_{up} > 100$, the machine body tilts.

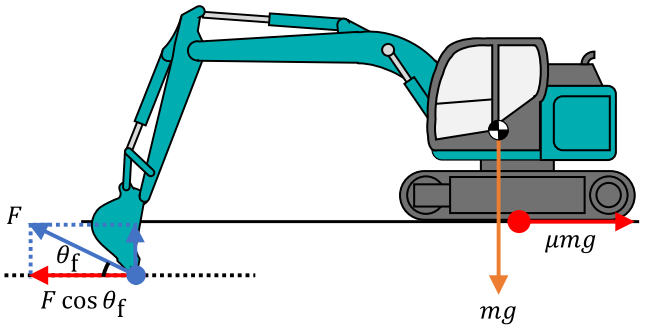

FIGURE 4. Horizontal forces.

B. FORWARD INSTABILITY

As shown in Fig. 4, considering the force in the horizontal direction, the maximum static friction force F_m is given by

$$F_m = \mu mg \tag{4}$$

where μ is the coefficient of static friction between the machine and ground.

The force F_b caused by the digging reaction force is given by

$$F_b = F\cos\theta_f. \tag{5}$$

From (4) and (5), the condition under which the machine is dragged forward is $F_b > F_m$. Based on this, the forward instability I_{for} (%) is defined as

$$I_{for} = \frac{F_b}{F_m} \cdot 100. \tag{6}$$

If $I_{for} > 100$, the machine body will be dragged forward.

C. MACHINE INSTABILITY

From (3) and (6), the machine instability I (%) is defined as

$$I = \begin{cases} I_{up} & (I_{up} > I_{for}) \\ I_{for} & (\text{otherwise}). \end{cases} \tag{7}$$

This is an index of the excavator condition assuming that when the machine body starts to lift or drag forward, machine instability is 100%.

III. SIMULATOR EXPERIMENTS

A. SIMULATOR CONFIGURATION

First, an evaluation using a simulator was carried out to verify the effect of presenting machine instability. In previous research on the excavation simulator, Dopico *et al.* [26] developed a full 3D physics-based excavator simulator made up of 14 rigid bodies with 17 degrees of freedom and a terrain mesh model of soil. Ni *et al.* [27] developed a multiple display virtual reality system for the excavator simulator with a real-time optimally adapting mesh algorithm for producing terrain deformation. However, these simulators have a high calculation cost for simulating soil behavior. Therefore, we developed a new simulator specialized in digging operation with a low computational cost compared with these studies, according to the purpose of this study.

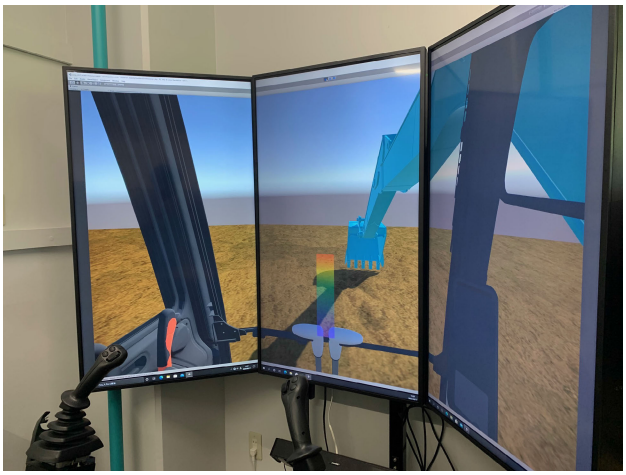

FIGURE 5. Excavator simulator appearance.

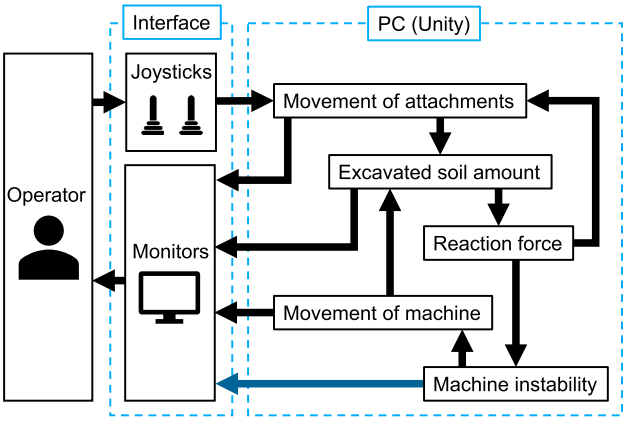

FIGURE 6. Schematic configuration of excavator simulator.

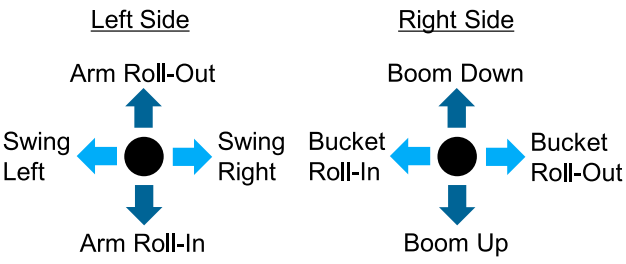

FIGURE 7. Excavator control pattern (ISO standard).

The excavator simulator is shown in Fig. 5, and the schematic configuration of the simulator is shown in Fig. 6. The simulator consisted of two joysticks, three monitors, and a PC; the simulation environment was created using a game engine, Unity. In the simulation environment, a 3D model simulating a 13t-class hydraulic excavator SK135SR-3 made by Kobelco Construction Machinery Co., Ltd. was arranged and rotated by 90°. The image displayed on the monitors was presented from the viewpoint of the actual excavator operation seat, and the joysticks were used in the same way as those of the actual hydraulic excavator. As shown in Fig. 7, the operating pattern conformed to the standards of the international organization for standardization (ISO). The turning motion, which is not used in the normal digging operation, is not simulated.

TABLE 1. Values for transfer function parameters.

Bucket Edge Position	Above the Ground			Below the Ground		
	K	T	L	K	T	L
Boom Up (Acceleration)	0.35	0.2	0.1	0.18	0.2	0.1
Boom Up (Deceleration)	0.35	0.1	0.1			
Boom Down	0.4	0.2	0.1			
Arm	0.56	0.2	0.1	K_A	0.2	0.1
Bucket	1.1	0.08	0.1	0.7	0.08	0.1

1) MOVEMENT OF ATTACHMENTS

The angular velocity of the attachment movement is changed according to the input from the joysticks, as in the actual excavator. The motion includes a response delay because the hydraulic excavator operates through a hydraulic circuit and cylinder. In this study, as proposed by Koiwai *et al.* [28], the dynamic characteristics $G(s)$ of the attachment were assumed to be a first-order plus dead time system as follows:

$$G(s) = \frac{K}{1+Ts} e^{-Ls} \tag{8}$$

where K is the system gain, T is the time constant, and L is the dead time. To approximate the movement of a general 13t-class hydraulic excavator, these values were assumed as shown in Table 1.

In the hydraulic excavator, the hydraulic pump is driven by the engine output, and it sends hydraulic oil to the hydraulic cylinder, which moves the attachment. When the load to the attachment increases, the amount of oil discharged from the hydraulic pump is controlled to prevent the engine output from exceeding the engine capacity and stall, and the attachment operation speed decreases. Therefore, to improve the reproducibility, the parameters were changed when the bucket tip was above the ground (i.e., no digging reaction force) and below the ground (i.e., digging reaction force exists). Additionally, because the ratio of the arm motion is larger than that of the other motions when digging, the gain K_A of the arm motion when the bucket tip is below the ground is changed, according to the digging reaction force, to improve the reproducibility of the arm motion. In this study, the angular velocity is assumed to decrease linearly as the digging reaction force increases, and K_A is defined as follows:

$$K_A = \begin{cases} K_{Amax} \cdot \dfrac{F_{max} - F}{F_{max}} & (F < F_{max}) \\ 0 & (\text{otherwise}) \end{cases} \tag{9}$$

where K_{Amax} is the maximum value of the gain, and F_{max} is the digging reaction force with zero gain. In this study, K_{Amax} was 0.56 and F_{max} was 55 kN.

2) CALCULATION AND DISPLAY METHOD OF EXCAVATED SOIL VOLUME

To calculate the digging reaction force and set the goal in the task of the simulator experiment, the excavated soil volume was calculated from the trajectory of the bucket

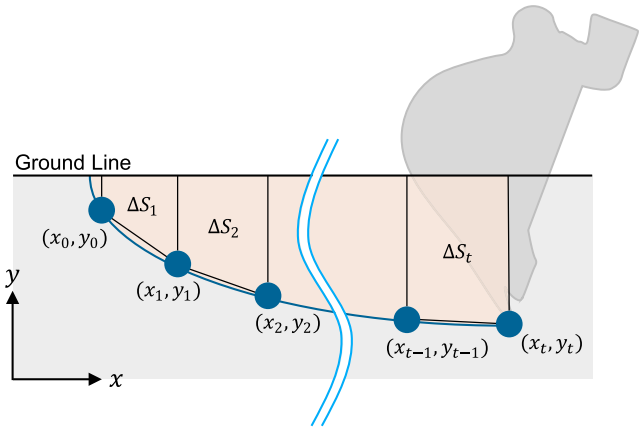

FIGURE 8. Excavated soil volume calculation.

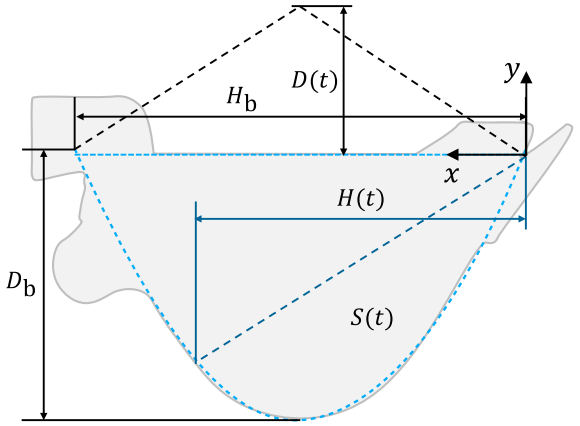

FIGURE 9. Display method of excavated soil in bucket.

tip, and a system for displaying the excavated soil in the bucket was applied. The excavated soil volume was calculated using the area surrounded by the trajectory of the bucket tip and the ground. As shown in Fig. 8, assuming that the position of the bucket tip at an arbitrary time t is (x_t, y_t), the bucket passing area $S(t)$ is as follows:

$$S(t) = \sum_{i=1}^{t} \Delta S_i, \tag{10}$$

$$\Delta S_i = \begin{cases} \frac{1}{2}|x_i - x_{i-1}|(|y_i| + |y_{i-1}|) & (x_i > x_{i-1} \wedge y_i < 0) \\ 0 & (\text{otherwise}). \end{cases} \tag{11}$$

In the actual digging work, the excavated soil volume is less than the volume of the bucket passing area because not all of the excavated soil enters the bucket. Therefore, the excavated soil volume $V(t)$ was calculated as

$$V(t) = S(t) W_b k_v \tag{12}$$

where k_v is the ratio of the excavated soil volume to the volume of the bucket passing area, and W_b is the bucket width and assumed to be constant.

Here, we describe the manner in which the excavated soil is displayed. The bucket section is approximated by a quadratic function. In the $x - y$ coordinates shown in Fig. 9, the bucket section is given by

$$y = \frac{4\, D_b}{{H_b}^2}\left(x - \frac{H_b}{2}\right) - D_b \tag{13}$$

where H_b is the bucket opening height, and D_b is the bucket depth. Assuming that the excavated soil volume increases in the bucket, as shown in Fig. 9, the bucket soil height $H(t)$ for the excavated soil volume until the bucket is full is

$$H(t) = \sqrt[3]{\frac{3{H_b}^2\, V(t)}{2\, D_b W_b}}. \tag{14}$$

After the bucket is full, the soil assumes the shape of a square pyramid, and its height increases, as shown in Fig. 9; the display height $D(t)$ is

$$D(t) = \frac{3}{W_b H_b}\left(V(t) - \frac{2}{3} D_b H_b W_b\right). \tag{15}$$

3) DIGGING REACTION FORCE

The digging reaction force is calculated using the attachment posture and the bucket soil height calculated using (14). Osumi *et al.* [29] and Meng *et al.* [30] proposed an estimation method for the digging reaction force using passive earth pressure. The passive earth pressure is the earth pressure generated on the retaining wall that supports sand; the theoretical formula was proposed by Coulomb and Rankine, wherein the digging reaction force was calculated using the Rankine theory [31]. The theoretical formula of the passive earth pressure F_p based on the Rankine theory is

$$F_p = \frac{1}{2}\gamma h^2 \tan^2\left(45^\circ + \frac{\varphi}{2}\right) \tag{16}$$

where h is the retaining wall height, γ is the unit weight of the soil, and φ is the internal friction angle. γ and φ are parameters determined by the soil properties. In this study, the retaining wall height was determined as $h_s(t)$ of the bucket soil height perpendicular to the ground, as shown in Fig. 10. The angle between the bucket opening surface and the bucket soil surface, $\theta_s(t)$, is

$$\theta_s(t) = \begin{cases} \tan^{-1} \dfrac{D_b - \dfrac{4\, D_b}{H_b}\left(H(t) - \dfrac{H_b}{2}\right)^2}{H(t)} & (H(t) < H_b) \\ 0 & (\text{otherwise}). \end{cases} \tag{17}$$

Assuming that the angle between the bucket opening surface and the ground surface is θ_{BG}, $h_s(t)$ is

$$h_s(t) = \frac{H(t)}{\cos\theta_s(t)} \sin(\theta_s + \theta_{BG}). \tag{18}$$

In the actual work, the soil inside the bucket is assumed to be loose. Assuming that the ratio of the height functioning as a retaining wall to $h_s(t)$ is k_s, the digging reaction force $F(t)$ is

$$F(t) = \frac{1}{2}\gamma h_s^2(t)\, k_s \tan^2\left(45^\circ + \frac{\varphi}{2}\right). \tag{19}$$

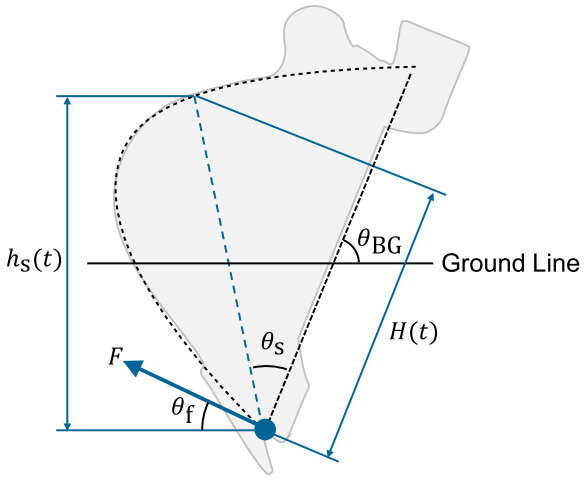

FIGURE 10. Digging reaction force calculation.

TABLE 2. Values for soil parameter.

Soil Pattern	γ [kN/m^3]	φ [°]
1	23	45
2	22	44
3	21	43

In this study, the digging reaction force was applied to the bucket tip, and the angle was set to 90° from the bucket opening surface.

4) MOVEMENT OF MACHINE

To reproduce the behavior of the machine during lifting and dragging forward, when the machine instability exceeds 100%, the machine is rotated and moved in the reverse direction of the change in the bucket tip position that is calculated from the input. Thus, although the absolute position of the bucket tip does not change, and the machine angle and position are changed.

B. EXPERIMENTS

1) CONDITION AND PROTOCOL

To confirm the effect of presenting the machine instability, a subject test using the simulator was conducted. Two conditions were tested (with and without machine instability feedback), and in each case, three different soil parameter conditions were used 10 times each for 30 digging trials. In actual digging, it is difficult to determine the conditions below the soil surface before digging. To simulate this situation, the trial order of the soil parameter conditions was randomized. The soil parameter conditions are given in Table 2. The soil property is assumed to be constant, and the parameters of the soil patterns are set so that a difference in the difficulty of tasks occurs with reference to type (cohesionless gravels) and soil description (very dense) based on [32]. According to (16), the digging reaction force against the retaining wall height decreases in the order of soil patterns 1, 2, and 3, which is an easy trial. In this study, μ was 0.35, k_v was 0.625, and k_s was 0.667.

The test task was to dig a specified amount of soil assuming a full bucket. Assuming that the full bucket has a 20% increase in capacity, for a bucket of 0.5 m^3 capacity, 0.6 m^3 was set as the target excavated soil volume. When the excavated soil volume reached the target excavated soil volume, the color of the excavated soil was changed to green, and the subject was informed that the target excavated soil volume had been reached. The purpose of setting the target excavated soil volume was to reduce the difference in excavated soil volume between tasks and subjects, and the data were not excluded for the trial when the target excavated soil volume was not reached.

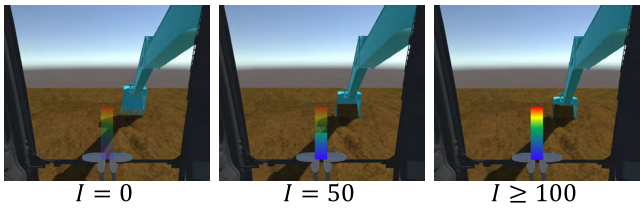

FIGURE 11. Machine instability meter for simulator experiments.

The machine angle, position, machine instability, excavated soil volume, and task time were measured. The task time started when either lever operation was input, and ended when the bucket tip was lifted more than 1 m after digging.

The subjects were 10 healthy adult males aged 29 to 54 years with hydraulic excavator operating experience. To eliminate the effect of trial order, five subjects performed the task with the feedback of the machine instability first, and the remaining five subjects performed the task without the feedback first. All subjects performed the task after practice under the condition of soil pattern 2 and without the feedback. Each subject was instructed to perform digging work on the target excavated soil volume as rapidly as possible. The subjects were informed beforehand that on the machine instability feedback meter, a 100% level indicates the start of machine motion. Informed consent based on the Declaration of Helsinki was obtained from all participants prior to the experiments.

2) METHOD FOR PROVIDING MACHINE INSTABILITY FEEDBACK

The machine instability meter is as shown in Fig. 11. The meter position was to the left of the bucket, and when the machine instability was 0%, it was displayed with a translucent pattern and became nontransparent from the bottom according to the magnitude of the machine instability. The ratio displayed in the nontransparent pattern was the same as that of the machine instability. The threshold value was set at 100%, and the meter became completely nontransparent when the machine instability exceeded the threshold value.

3) RESULTS

The experimental results were evaluated in terms of productivity and safety. Each index refers to the mean value per subject for each condition and soil pattern. "Without F/B" in the figure means the case without machine instability feedback, and "With Machine Instability F/B" means the

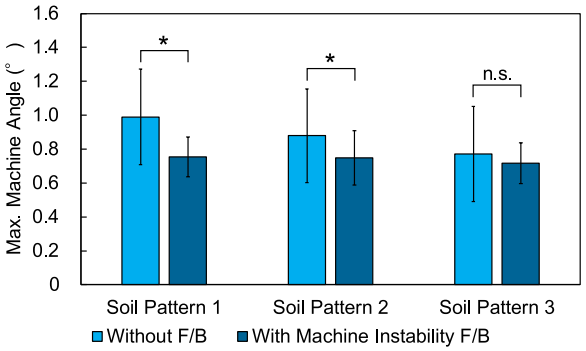

FIGURE 12. Differences in mean values of maximum machine angle for simulation experiment. Error bars indicate standard deviation. Asterisks indicate significant differences (*$p < .05$). Hypothesis for student's t-test is value of "Without F/B" greater than value of "With Machine Instability F/B."

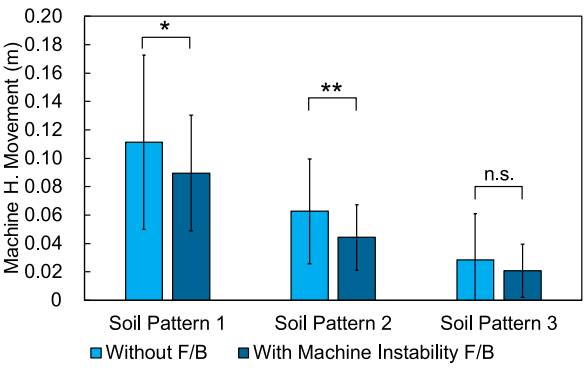

FIGURE 13. Differences in mean values of horizontal machine movement for simulation experiment. Error bars indicate standard deviation. Asterisks indicate significant differences (*$p < .05$, **$p < .01$). Hypothesis for student's t-test is value of "Without F/B" greater than value of "With Machine Instability F/B."

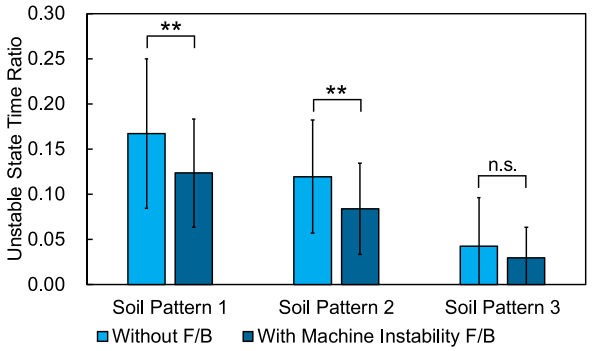

FIGURE 14. Differences in mean values of unstable state time ratio for simulation experiment. Error bars indicate standard deviation. Asterisks indicate significant differences (**$p < .01$). Hypothesis for student's t-test is value of "Without F/B" greater than value of "With Machine Instability F/B."

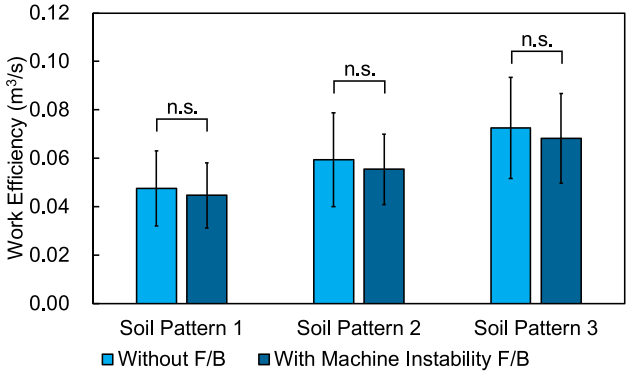

FIGURE 15. Differences in mean values of work efficiency for simulation experiment. Error bars indicate standard deviation.

case with machine instability feedback. A p-value of less than 0.05 was regarded as statistically significant.

Fig. 12 demonstrates the mean of the maximum machine angle in one task. Student's t-test indicates that the maximum machine angle with machine instability feedback is significantly lower than that without machine instability feedback in the case of soil pattern 1 ($t(9) = 2.817, p = .010$) and soil pattern 2 ($t(9) = 2.058, p = .035$). No significant decrease was observed in the case of soil pattern 3 ($t(9) = 0.948$, $p = .184$) between the two conditions.

Fig. 13 shows the mean of the maximum horizontal movement in one task. Student's t-test indicates that the maximum horizontal movement with machine instability feedback is significantly lower than that without machine instability feedback in the case of soil pattern 1 ($t(9) = 2.001$, $p = .038$) and soil pattern 2 ($t(9) = 2.856, p = .009$). No significant decrease was observed in the case of soil pattern 3 ($t(9) = 0.874, p = .202$) between the two conditions.

Fig. 14 shows the mean of the unstable state time ratio obtained by dividing the time when the machine instability exceeds 100% by the task time. A smaller vertical axis value results in a shorter working time in the unstable state. Student's t-test indicates that the unstable state time ratio with machine instability feedback is significantly lower than that without machine instability feedback in the case of soil pattern 1 ($t(9) = 3.598, p = .003$) and soil pattern 2 ($t(9) = 2.905, p = .009$). No significant decrease was observed in the case of soil pattern 3 ($t(9) = 1.322, p = .109$) between the two conditions.

In terms of productivity, Fig. 15 shows the mean work efficiency obtained by dividing the excavated soil volume by the task time. Student's t-test was conducted for the condition with or without machine instability feedback; there were no significant differences in the case of soil pattern 1 ($t(9) = 1.577, p = .149$), soil pattern 2 ($t(9) = 1.725, p = .119$), and soil pattern 3 ($t(9) = 1.973, p = .080$).

4) DISCUSSION

The maximum machine angle, maximum horizontal movement, and unstable state time ratio showed significant decreases except for soil pattern 3. Therefore, it can be said that by presenting machine instability, the amount of movement of the machine and the time when the machine body was moving decreased. Soil pattern 3 was the easiest trial condition, and it was inferred that there was no difference because the machine instability rarely exceeded 100%, as shown in Fig. 14. Regarding productivity, there was no significant difference in work efficiency under any soil pattern; it is considered that the machine instability feedback did not reduce productivity. It was shown that by feeding back the

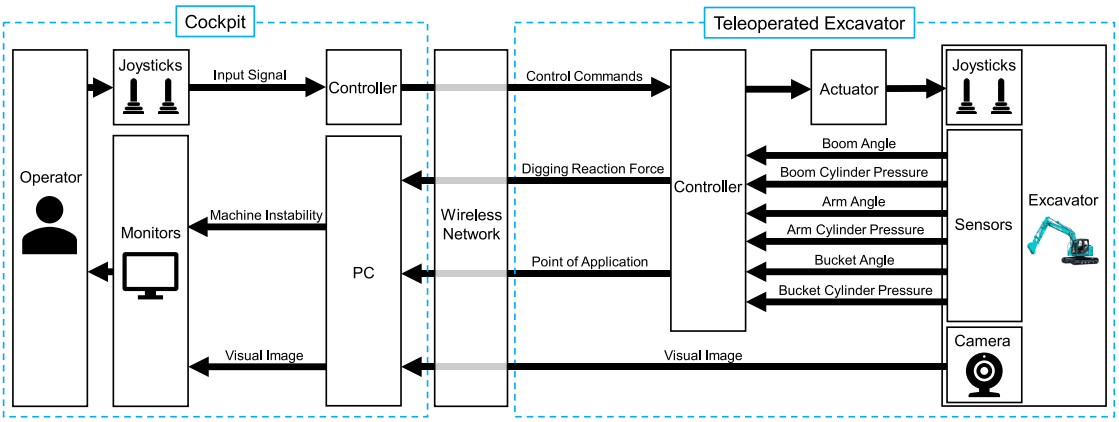

FIGURE 16. Schematic configuration of teleoperated excavator.

machine instability, digging work could be performed safely without reducing productivity. This comment was given: "When the machine instability becomes 100% or more, it is not possible to check by how much the instability exceeds 100%, so the extent to which the lever operation should be changed is not clear." after the trial. Therefore, in the experiment using the actual teleoperation excavator, the meter was changed.

IV. EXPERIMENTS WITH TELEOPERATED EXCAVATOR

A. TELEOPERATED EXCAVATOR CONFIGURATION

Next, to verify the effect of the machine instability feedback in an actual teleoperated excavator, a test was conducted. The schematic configuration of the teleoperated excavator used for the experiment is shown in Fig. 16. This is the modification of the one developed by the authors [6]; the list of modifications are follows:

- The hydraulic excavator changed from 7t-class to 13t-class (SK135SR-3).
- A digging reaction force measurement system was installed.
- The number of cameras was changed from two to one.
- Visual information was changed from the head mounted display to monitors.

According to the input of the joysticks by the operator, the joystick on the teleoperated excavator side is operated by the actuator. The operation method is the same as that of the simulator, as shown in Fig. 7. The digging reaction force and its point of application are calculated by the controller in the teleoperated excavator based on the values from the pressure sensors and angle sensors of the attachment. The system had a delay of about 160 ms from the input of joysticks of the cockpit to the output of the actuator of teleoperated excavator, about 60 ms from capturing of images by the camera to displaying them on the monitors, and about 50 ms from getting the sensor value to displaying the machine instability on the monitors. Because the purpose of this study was to verify the effect of the machine instability feedback, the motion simulator sheet was turned off. There are other changes in the components, but they were omitted because they deviate from the purpose of this study.

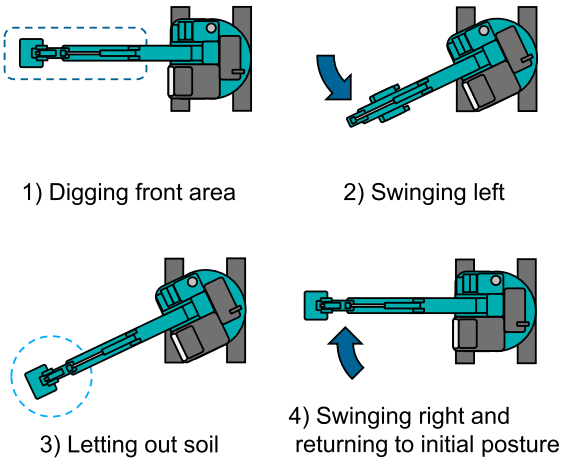

FIGURE 17. Experimental task (one set).

FIGURE 18. Actual image of teleoperated hydraulic excavator in experiment.

B. EXPERIMENTS

1) CONDITION AND PROTOCOL

To confirm the effect of presenting machine instability in an actual teleoperated excavator, a test was conducted. Two conditions (with and without machine instability feedback) were tested. In each case, two sets of five repetitions from task 1 to 4, as shown in Fig. 17, and a total of 10 digging works were performed by the subjects. The excavator was placed on horizontal ground and rotated by 90°, as shown in Fig. 18. In the experimental area, the behavior in which the machine was dragged forward during the digging work could not be reproduced. Therefore, the coefficient of static friction used for the calculation of the forward instability was set to 1.0.

FIGURE 19. Actual image of cockpit in experiment.

The machine angle, machine instability, excavated soil volume, and task time were measured. The machine angle was measured using an inertial measurement unit installed in the excavator body. To eliminate the effect of the initial machine angle, a high-pass filter with a cutoff frequency of 0.001 Hz was applied to the measured machine angle. The excavated soil volume was estimated from the vertical digging reaction force generated by the soil in the bucket during the turning operation after the digging work. The unit weight of soil used in the calculation was 22.0 kN/m^3. The task time started when the arm operation was input, and ended when the rotation operation was input.

The subjects were six healthy adult males aged 29 to 54 years with hydraulic excavator operating experience. To eliminate the effect of trial order, three subjects performed the task with the feedback of the machine instability first, and the remaining three subjects performed the task without the feedback first. All subjects performed the task after performing one set without the feedback. Each subject was instructed to perform digging with as much soil volume as possible and as rapidly as possible. The subjects were informed beforehand that on the machine instability feedback meter, a 100% level indicates the start of machine motion. Informed consent based on the Declaration of Helsinki was obtained from all participants before the experiments. A photograph of the cockpit during the test is shown in Fig. 19.

2) METHOD FOR PROVIDING MACHINE INSTABILITY FEEDBACK

The machine instability was displayed as a meter as in the simulator experiment. The meter used for the display is shown in Fig. 20. The threshold value was set at 100%, and the meter was changed to increase the nontransparent part when the machine instability exceeded the threshold, based on the comment after the simulator test.

3) RESULTS

The experimental results were evaluated in terms of productivity and safety. Each index refers to the mean value per subject for each condition and soil pattern. ''Without F/B'' in the figure means the case without machine instability feedback, and ''With Machine Instability F/B'' means the case with machine instability feedback. A p-value of less than 0.05 was regarded as statistically significant. The excavator was not dragged forward in any of the tasks.

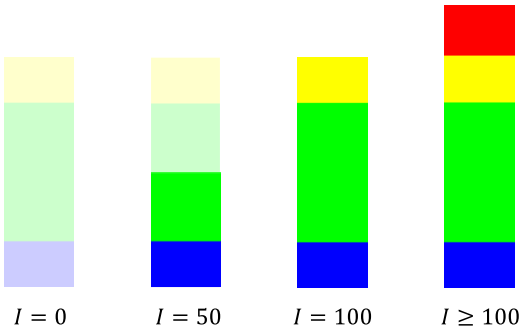

FIGURE 20. Machine instability meter for teleoperated excavator experiments.

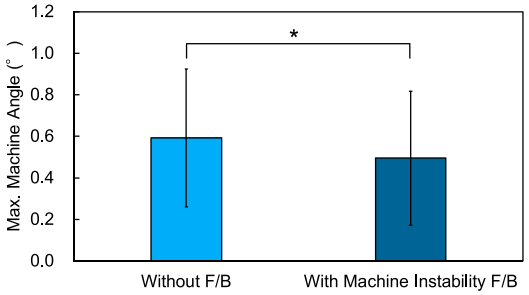

FIGURE 21. Differences in mean values of maximum machine angle for teleoperated excavator experiment. Error bars indicate standard deviation. Asterisks indicate significant differences (*p < .05). Hypothesis for student's t-test is value of "Without F/B" greater than value of "With Machine Instability F/B."

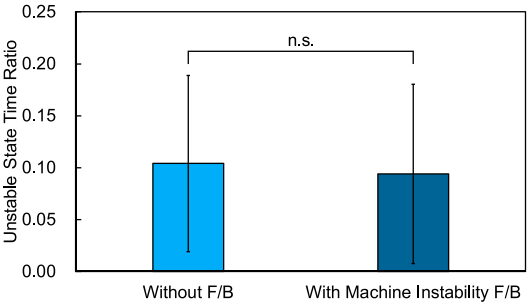

FIGURE 22. Differences in mean values of unstable state time ratio for teleoperated excavator experiment. Error bars indicate standard deviation. Hypothesis for student's t-test is value of "Without F/B" greater than value of "With Machine Instability F/B."

Fig. 21 shows the mean of the maximum machine angle in one task. Student's t-test indicates that the maximum machine angle with machine instability feedback is significantly lower than that without machine instability feedback ($t(5) = 2.094, p = .045$).

Fig. 22 shows the mean of the unstable state time ratio. Student's t-test indicates that there was no significant decrease between the two conditions ($t(5) = 0.704, p = .256$).

In terms of productivity, Fig. 23 shows the mean work efficiency. Student's t-test was conducted for the condition with or without machine instability feedback; there were no significant differences ($t(5) = 0.668, p = .534$).

4) DISCUSSION

Since a significant decrease in the maximum machine angle was confirmed, it can be said that the amount of movement

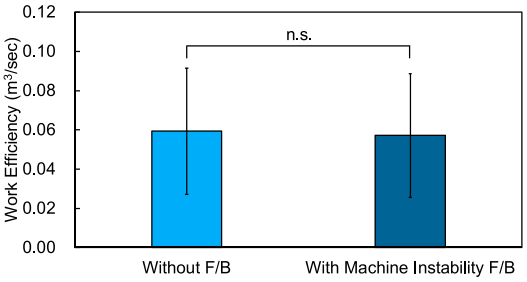

FIGURE 23. Differences in mean values of work efficiency for teleoperated excavator experiment. Error bars indicate standard deviation.

of the machine was reduced by presenting machine instability as in the experiment with the simulator. However, there was no significant decrease in the unstable state time ratio, indicating that the time at which the machine is moving has not decreased. The presumable reason was that the soil property was constant during one trial in the simulator, but the soil property was not uniform at the actual site. For example, when relatively large rocks or locally hard areas exist in the soil, the machine instability suddenly increases at those parts. Therefore, the adjustment of the operation was considered delayed, and the machine instability exceeded 100% occasionally. As an example, Fig. 24 shows the changes in machine angle, machine instability, and bucket tip height in the test with a certain subject. It can be observed that the machine instability suddenly changes after approximately 2 s, even though the bucket tip height does not change substantially. It is possible that the same phenomenon can be reproduced in the simulator by reproducing nonuniform soil and by modeling ground deformation.

Besides, as shown in Fig. 24, the time when the machine instability was exceeding 100% is almost the same as the time when the machine angle was relatively large. Therefore, it is considered that the machine instability can be sufficiently used as an index of the excavator condition.

Regarding productivity, there was no significant difference in work efficiency, so it is considered that the presentation of the machine instability did not degrade productivity, as in the simulator experiment.

From the above discussion, it was clarified that the digging work could be carried out without lowering the productivity and without generating the tilt of the machine by feeding back the machine instability.

V. GENERAL DISCUSSION

In this study, to improve the safety of the excavation by a teleoperated excavator, machine instability, which is an index of the excavator condition with the condition when the excavator body starts to move is assumed to be 100%, was proposed; as a method for feeding back the machine instability to the operator, a visual presentation method using a meter that can intuitively represent the index was introduced. To confirm the effect of this machine instability feedback, experiments using a simulator and an actual teleoperated excavator were conducted. The results of the simulator test

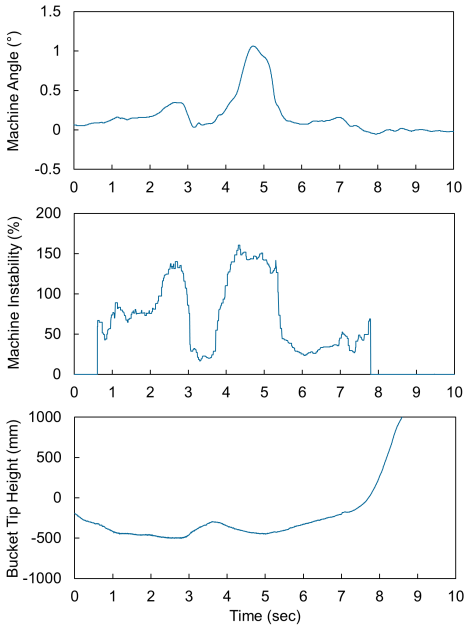

FIGURE 24. Time series graph of machine angle, machine instability, and bucket tip height in one excavation for teleoperated excavator experiment.

demonstrated the possibility of performing the excavation safely without lowering the productivity using the machine instability feedback. In addition, the results of the experiment using an actual teleoperated excavator confirmed that, with the machine instability feedback, it was possible to excavate without lowering productivity and without increasing the tilt of the excavator.

Regarding safety, when there is no feedback, it is necessary to estimate the load margin only from the information received from images. However, it is considered that this result was obtained because it is possible to intuitively determine the load margin due to the machine instability feedback. In this study, only the horizontal ground test was conducted; however, a large effect is expected on slopes where it is more dangerous and difficult for the operator to obtain the tilt angle of the teleoperated excavator because the load margin can be intuitively obtained.

Regarding productivity, it was confirmed that machine instability feedback had no adverse effect. In a previous study by Lécuyer *et al.* [33], the effect of additional feedback information by haptic, visual, and auditory information on the performance of the operator was investigated. For the task of manipulating the ball and inserting it into the openings in the five walls in order, as a result of feeding back the magnitude of the reaction force acting when the ball collides with the wall, it is reported that the task time increased because the operation involving feedback was considered more prudent than the case without the feedback in any condition. However, this study does not demonstrate a decrease in work efficiency. It is considered that this is the effect of providing feedback regarding load margin, that is, providing feedback that the condition is becoming unfavorable as compared to providing feedback on whether the unfavorable condition occurs or not.

This machine instability is different from force feedback and tactile feedback in previous studies and is considered to be more effective for the safety of teleoperation because the operator can directly obtain the load margin of the machine. In addition, there was a delay in the actual teleoperated excavator experiment, it is necessary to further clarify how the delay affects the effect of the proposed method.

Further improvement is necessary in the method of machine instability feedback. In the experiment using the teleoperated excavator, there was no significant difference in the unstable state time ratio. This is because the operator cannot make timely adjustments with respect to the rising rate of change exhibited by the meter. To solve this problem, it is necessary to consider the display method, such as setting the threshold of the meter to less than 100%. In addition, after both the simulation and the teleoperated excavator experiments, a few subjects commented that it was difficult to dig while looking at both the meter and the bucket. There is a possibility that the visual and psychological loads increase with the machine instability feedback. To solve this problem, it is necessary to consider the meter position and the use of non-visual feedback such as sound and vibration.

The limitation of this study is that the verification of the forward instability has not been conducted in an actual teleoperated excavator. Although the situation where the excavator was dragged forward could not be reproduced in the experimental site, it is considered that additional verification is necessary because the behavior may occur with the soil condition and the tilt angle of the ground.

VI. CONCLUSION

In this study, to examine the safety improvement and the effect on the work performance in excavation by the teleoperated excavator, the machine instability derived from the attachment posture and the digging reaction force was proposed, considering the extent of load at which the excavator body starts to move. In addition, a visual presentation method using a meter capable of intuitively representing the index as a method for feeding back the machine instability to the operator was proposed. To verify the effect of the machine instability feedback, an excavation operation simulator was constructed, and an experiment was conducted. As a result, it was confirmed that the work could be conducted without generating the tilting and forward movement of the machine body, and that the ratio of the time when the machine instability exceeded 100% decreased, while the productivity remained constant. In addition, as a result of verifying the effect of the subject experiment even in the actual teleoperated excavator, it was confirmed that the work could be conducted without causing the machine to tilt more, while the productivity was maintained. From the results, it was confirmed that safer work could be conducted without using expensive and large output actuators in the teleoperated excavator in which the machine posture is difficult to obtain, using the machine instability feedback. In the future, it would be of interest to further re-examine the display method and the position of the machine instability meter, as well as to consider methods of providing additional non-visual feedback to the operator. Besides, the proposed machine instability may be used to assist the operation of hydraulic excavators.

REFERENCES

[1] H. Sulaiman, M. N. A. Saadun, and A. A. Yusof, "Modern manned, unmanned and teleoperated excavator system," *J. Mech. Eng. Tech*, vol. 7, no. 1, pp. 57–68, 2015.

[2] M. Moteki, K. Fujino, T. Ohtsuki, and T. Hashimoto, "Research on visual point of operator in remote control of construction machinery," in *Proc. 28th Int. Symp. Autom. Robot. Construct. (ISARC)*, Jun. 2011, pp. 532–537.

[3] M. Moteki, K. Fujino, and A. Nishiyama, "Research on Operator's mastery of unmanned construction," in *Proc. 30th Int. Symp. Autom. Robot. Construction Mining (ISARC), Building Future Autom. Robot.*, Aug. 2013, pp. 540–547.

[4] Y. Sakaida, D. Chugo, H. Yamamoto, and H. Asama, "The analysis of excavator operation by skillful operator–extraction of common skills -," in *Proc. SICE Annu. Conf.*, Aug. 2008, pp. 538–542.

[5] D. Zhao, Y. Xia, H. Yamada, and T. Muto, "Control method for realistic motion in a construction tele-robotic system with a 3-DOF parallel mechanism," *J. Robot. Mechtron.*, vol. 15, no. 4, pp. 361–368, Aug. 2003, doi: 10.20965/jrm.2003.p0361.

[6] M. Ito, Y. Funahara, S. Saiki, Y. Yamazaki, and Y. Kurita, "Development of a cross-platform cockpit for simulated and tele-operated excavators," *J. Robot. Mechtron.*, vol. 31, no. 2, pp. 231–239, Apr. 2019, doi: 10.20965/jrm.2019.p0231.

[7] N. R. Parker, S. E. Salcudean, and P. D. Lawrence, "Application of force feedback to heavy duty hydraulic machines," in *Proc. IEEE Int. Conf. Robot. Autom.*, May 1993, pp. 375–381.

[8] P. D. Lawrence, S. E. Salcudean, N. Sepehri, D. Chan, S. Bachmann, N. Parker, M. Zhu, and R. Frenette, "Coordinated and force-feedback control of hydraulic excavators," in *Experimental Robotics IV*, O. Khatib and J. K. Salisbury, Eds., 1st ed. Berlin, Germany: Springer, 1997, pp. 181–194.

[9] K. Ahn, "Development of force reflecting joystick for hydraulic excavator," *JSME Int. J. Ser. C*, vol. 47, no. 3, pp. 858–863, 2004, doi: 10.1299/jsmec.47.858.

[10] X. Li, "Study on master-slave control method using load force and impedance identifiers for tele-operated hydraulic construction robot," *Appl. Mech. Mater.*, vols. 29–32, pp. 2170–2175, Aug. 2010, doi: 10.4028/www.scientific.net/AMM.29-32.2170.

[11] D. Q. Truong, B. N. M. Truong, N. T. Trung, S. A. Nahian, and K. K. Ahn, "Force reflecting joystick control for applications to bilateral teleoperation in construction machinery," *Int. J. Precis. Eng. Manuf.*, vol. 18, no. 3, pp. 301–315, Mar. 2017, doi: 10.1007/s12541-017-0038-z.

[12] G. Mingde, Y. Bin, and Y. Hironao, "Performance experiment of a hydraulic force feedback teleoperation robot based on position and rate control," in *Proc. 2nd Int. Conf. Intell. Hum.-Mach. Syst. Cybern.*, Aug. 2010, pp. 87–90.

[13] J. Hou and D. Zhao, "A new force feedback algorithm for hydraulic teleoperation robot," in *Proc. Int. Conf. Comput. Appl. Syst. Model. (ICCASM)*, Oct. 2010, pp. V15-15–V15-18.

[14] L. Huang, T. Kawamura, and H. Yamada, "Construction robot operation system with Object's hardness recognition using force feedback and virtual reality," *J. Robot. Mechtron.*, vol. 24, no. 6, pp. 958–966, Dec. 2012, doi: 10.20965/jrm.2012.p0958.

[15] K. Zareinia and N. Sepehri, "A hybrid haptic sensation for teleoperation of hydraulic manipulators," *J. Dyn. Syst., Meas., Control*, vol. 137, no. 9, Sep. 2015, Art. no. 091001, doi: 10.1115/1.4030337.

[16] S. Lampinen and J. Koivumäki, and J. Mattila, "Full-dynamics-based bilateral teleoperation of hydraulic robotic manipulators," in *Proc. IEEE Int. Conf. Autom. Sci. Eng.*, Munich, Germany, Aug. 2018, pp. 1343–1350.

[17] L. Carvalho, P. Rezeck, M. V. Lima, L. Pinto, G. Freitas, E. R. Nascimento, D. G. Macharet, L. Chaimowicz, G. Pessin, and M. F. M. Campos, "On the evaluation of force feedback augmented teleoperation of excavator-like mobile manipulators," in *Proc. IEEE 16th Int. Conf. Autom. Sci. Eng. (CASE)*, Aug. 2020, pp. 1401–1407.

[18] K. Hayashi and T. Tamura, "Teleoperation performance using excavator with tactile feedback," in *Proc. Int. Conf. Mechatronics Autom.*, Aug. 2009, pp. 2759–2764.

[19] D. Kim, K. W. Oh, C. S. Lee, and D. Hong, "Novel design of haptic devices for bilateral teleoperated excavators using the wave-variable method," *Int. J. Precis. Eng. Manuf.*, vol. 14, no. 2, pp. 223–230, Jan. 2013, doi: 10.1007/s12541-013-0031-0.
[20] J. M. Jacinto-Villegas, M. Satler, A. Filippeschi, M. Bergamasco, M. Ragaglia, A. Argiolas, M. Niccolini, and C. A. Avizzano, "A novel wearable haptic controller for teleoperating robotic platforms," *IEEE Robot. Autom. Lett.*, vol. 2, no. 4, pp. 2072–2079, Oct. 2017, doi: 10.1109/LRA.2017.2720850.
[21] H. Nagano, H. Takenouchi, N. Cao, M. Konyo, and S. Tadokoro, "Tactile feedback system of high-frequency vibration signals for supporting delicate teleoperation of construction robots," *Adv. Robot.*, vol. 34, no. 11, pp. 730–743, Jun. 2020, doi: 10.1080/01691864.2020.1769725.
[22] T. Tanimoto, K. Shinohara, and H. Yoshinada, "Research on effective teleoperation of construction machinery fusing manual and automatic operation," *Robomech J.*, vol. 4, no. 1, pp. 1–12, Dec. 2017, doi: 10.1186/s40648-017-0083-5.
[23] B.-H. Yu, K.-Y. Park, K.-D. Lee, and C.-S. Han, "Static compensation ZMP algorithm preventing tips-over of a tele-operation excavator," in *Proc. ISG*ISARC Full Paper*, Jun. 2012, pp. 652–659.
[24] K. Shigematsu, T. Tsubouchi, and S. Sarata, "Tip-over prevention control of a teleoperated excavator based on ZMP prediction," in *Proc. IEEE Int. Conf. Autom. Sci. Eng. (CASE)*, Aug. 2016, pp. 1380–1386.
[25] M. Ito, C. Raima, S. Saiki, Y. Yamazaki, and Y. Kurita, "A study on machine instability feedback during digging operation in teleoperated excavators," in *Proc. 13th Int. Conf. Hum. Syst. Interact. (HSI)*, Jun. 2020, pp. 14–19.
[26] D. Dopico, S. Mendizabal, and M. González, "A soil model for a hydraulic simulator excavator based on real-time multibody dynamics," in *Proc. Asian Conf. Multibody Dyn.*, Kyoto, Japan, 2010, pp. 325–333.
[27] T. Ni, H. Zhang, C. Yu, D. Zhao, and S. Liu, "Design of highly realistic virtual environment for excavator simulator," *Comput. Electr. Eng.*, vol. 39, no. 7, pp. 2112–2123, Oct. 2013, doi: 10.1016/j.compeleceng.2013.06.010.
[28] K. Koiwai, R. Miyazaki, T. Yamamoto, K. Ueda, K. Yamashita, and Y. Yamazaki, "Responsiveness evaluation index for an excavator operation based on control engineering approach," *IEEJ Trans. Electron., Inf. Syst.*, vol. 138, no. 5, pp. 506–511, May 2018, doi: 10.1541/ieejeiss.138.506.
[29] H. Osumi, T. Uehara, N. Okada, T. Fujiwara, and S. Sarata, "Efficient scooping of rocks by autonomous controlled wheel loader," *J. Robot. Mechatronics*, vol. 24, no. 6, pp. 924–932, Dec. 2012, doi: 10.20965/jrm.2012.p0924.
[30] Y. Meng, H. Fang, G. Liang, Q. Gu, and L. Liu, "Bucket trajectory optimization under the automatic scooping of LHD," *Energies*, vol. 12, no. 20, p. 3919, Oct. 2019, doi: 10.3390/en12203919.
[31] W. J. M. Rankine, "On the stability of loose Earth," *Philos. Trans. R. Soc. Lond.*, vol. 147, pp. 9–27, Dec. 1857.
[32] B. G. Look, "Soil properties and state of the soil," in *Handbook of Geotechnical Investigation and Design Tables*, 1st ed. London, U.K.: Taylor & Francis, 2007, pp. 77–90.
[33] A. Lécuyer, C. Mégard, J. M. Burkhardt, T. Lim, S. Coquillart, P. Coiffet, and L. Graux, "The effect of haptic, visual and auditory feedback on an insertion task on a 2-screen workbench," in *Proc. Immers. Proj. Tech. Symp.*, 2002, pp. 1–9.

MASARU ITO received the M.E. degree in mechanical engineering from Kumamoto University, Kumamoto, Japan, in 2010.

In 2010, he joined Kobelco Construction Machinery Company Ltd., Hiroshima, Japan. Since 2017, he has been an Assistant Professor with the Next Generation Human Interface Collaborative Research Laboratory, Hiroshima University, Hiroshima. His research interests include human interface, control engineering, and mechatronics.

Prof. Ito is a member of the Japan Society of Mechanical Engineers and the Society of Instrument and Control Engineers.

CHIAKI RAIMA received the B.L.A., M.A.S., and Ph.D. degrees from Hiroshima University, Hiroshima, Japan, in 2014, 2016, and 2019, respectively.

From 2019 to 2020, she was a Researcher with the Kobelco Construction Machinery Dream-Driven Co-Creation Research Center, Hiroshima University, where she has been a Specially Appointed Assistant Professor, since 2020. Her research interest includes psychology about motor-skilled humans.

Dr. Raima is a member of the Japan Society of Mechanical Engineers.

SEIJI SAIKI joined Kobelco Construction Machinery Company Ltd., Hiroshima, Japan, in 2009. He is currently the Manager of the DX Consulting Group, Business Development Department, Kobelco Construction Machinery Company Ltd., Tokyo, Japan.

YOICHIRO YAMAZAKI received the M.E. degree in mechanical engineering from Ehime University, Ehime, Japan, in 1992.

From 1992 to 1999, he was working with Kobe Steel, Ltd. In 1999, he joined Kobelco Construction Machinery Company Ltd., Hiroshima, Japan. Since 2019, he has been a Visiting Professor with Hiroshima University, Hiroshima. He is currently the General Manager of the Business Development Department, Kobelco Construction Machinery Company Ltd., Tokyo, Japan.

Prof. Yamazaki is a member of the Japan Society of Mechanical Engineers.

YUICHI KURITA (Member, IEEE) received the B.E. degree from Osaka University, Osaka, Japan, in 2000, and the M.E. and Ph.D. degrees in information science from the Nara Institute of Science and Technology (NAIST), Nara, Japan, in 2002 and 2004, respectively.

From 2005 to 2007, he was a Research Associate with the Graduate School of Engineering, Hiroshima University, Hiroshima, Japan. From 2007 to 2011, he was an Assistant Professor with the Graduate School of Information Science, NAIST. From 2010 to 2011, he was a Visiting Scholar with the School of Mechanical Engineering, Georgia Institute of Technology, Georgia, USA. In 2011, he joined the Graduate School of Advanced Science and Engineering, Hiroshima University, as an Associate Professor, where he has been a Professor, since 2018. His research interests include physical human–robot interaction (pHRI), human augmentation, haptics, and medical engineering.

Dr. Kurita is a member of the Japan Society of Mechanical Engineers, the Robotics Society of Japan, the Virtual Reality Society of Japan, and the Society of Instrument and Control Engineers.